

## Optimal Backstepping Controller Design for Prosthetic Knee Joint

Mayyasah Ali Salman\*, Saleem Khalefa Kadhim

Control and System Engineering Department, University of Technology-Iraq, Baghdad 10066, Iraq

Corresponding Author Email: [cse.19.18@grad.uotechnology.edu.iq](mailto:cse.19.18@grad.uotechnology.edu.iq)



<https://doi.org/10.18280/jesa.550105>

### ABSTRACT

**Received:** 13 October 2021

**Accepted:** 13 January 2022

#### Keywords:

*prosthetic knee, backstepping control, bat algorithms, Lyapunov theory*

The mobility of people who have had a lower limb amputated is slower, less stable, and needs more metabolic energy than the movement of physically fit, also, often have difficulty moving on uneven terrain and stairs. In most cases, these problems may be traced back to the usage of controllers for an above-knee prosthesis, which enhances movement and more quality of life for millions of individuals who have lost lower limbs. In this work addresses the dynamic modeling and parameter identification of the lower limb, and the control of a 2-DOF joint prosthetic, because the uncertainty, high nonlinearity, problems with imbalance, and external perturbations, which can occur during movement. Backstepping control algorithm based on the Lyapunov theory was used, this is to ensure system stability with enhanced dynamic performance. The Bat algorithms optimization technique was used to fine-tune these design parameters to improve the performance of the proposed controller. From the results, found that the quantitative comparison between the present study and the related articles previously published which used sliding mode observer control, showed reasonable agreement. To comparison between convolution Backstepping control and optimal Backstepping control with Bat algorithms, at the control action consumptions. It was found that the position error of the prosthetic knee is enhanced by 9% at joint1 and 7.4% at joint2, respectively. Therefore, the results are considered satisfactory for such biomedical systems.

## 1. INTRODUCTION

Due to conflict, sickness, traffic accidents, and natural disasters, millions of people have had difficulty using their lower limbs in recent decades. As a result, some of them have lost their ability to work and are unable to participate in normal social activities [1]. The tools available to people who lost their lower limbs were walkers, wheelchairs, wooden braces, and crutches. Nowadays, advances in medical science and technology can be used to help people with amputations using motorized lower limbs [2]. Their quality of life is severely reduced as a result of their physical and mental limitations, which puts them under a great deal of physical and mental strain. People who have lost limbs must rely on prosthetics to compensate for their loss because present medical technology does not allow for the regeneration of limbs. Conventional mechanistic knee prostheses can't make a big difference within the lives of amputees due to their incorrect walking, massive bodily effort, and terrible affected person sporting experience. A range of rehabilitative robots were advanced to assist and repair human mobility due to strength storage, advances in actuation, tiny sensing, micro embedded pc technology, and automatic sample recognition [3, 4]. There are many difficult problems such as system uncertainty, high nonlinearity, and external perturbations, which can occur during movement, problems with imbalance, falls and sudden bending of the knee while standing. Since there are many control strategies used to control the movement of prosthetic limbs, including Backstepping Control (BC). The BC is based on a control strategy for a certain sort of nonlinear systems. Due to its ability to handle the nonlinearity and uncertainty

with high efficiency. The Lyapunov theory combined with BC improves the closed-loop system's dynamic performance while also ensuring its stability.

For the design of BC, first the error equations are derived, and the equations of the system are then supplemented with an additional state based on the integration of the error. The system equations are separated into subsystems so that the controller can be designed iteratively. Based on the Lyapunov function, a virtual control signal is chosen for each stabilizing subsystem. All system equations are evaluated in the final design process, and the control signal is created in such a way that the closed loop system is stable according to Lyapunov theory [5]. Also, there are many researchers who have suggested some strategies for controlling prosthetic limbs.

Azimi et al. [6] introduced two strong model-based controllers for artificial transfemoral gait: the Robust Passive controller (RP), and the Robust glide mode (RS). Both controllers for continuous dynamics are proven to be stable under the Lyapunov stability theory. The results show that for a healthy person wearing a transfemoral prosthesis, both controllers give human-like gait and accurate tracking.

Scandaroli et al. [7] presented a design a prosthetic limb above the knee. Proportional-Integral-Derivative (PID) and model references Adaptive controllers are used in their models. They found that the results revealed difficulty in controlling such a nonlinear plant.

Mefoued and Belkhiat [8] proposed a Sliding Mode Observer (SMO) based powerful control to leading an exoskeleton has been developed to help persons who have limited knee movement. A SMO has been constructed and inserted into the closed loop of the system to provide velocity.

The stability of a system can be proven using Lyapunov's theory. In their model, they compare between SMO and PID controller, found that the SMO method guarantees the excellent overall performance in terms of stability, location tracking, speed control and disturbance rejecting capability.

Wen et al. [9] presented Adaptive Dynamic Programming (ADP) based controller performance testing that automatically configures prosthetic control parameters. The system was evaluated on a physically healthy person, walking with an electrical prosthesis on a treadmill. The goal was for the user to be able to approximate conventional knee kinematics using ADP to alter the Finite State Impedance Control (FSIC) resistance values. They tested the practicality of ADP for adaptive control of a powered prosthesis and discovered that in about 10 minutes, the prosthetic controller could be tuned to provide modular kinematics of the knee.

Martinez-Villalpando and Herr et al. [10] provided design and execution of a knee prosthesis with two parallel series elastic actuators. The parameters of the model were changed using an optimization scheme, and then they utilized these optimized values to define the mechanical and control design of the prosthesis. In their model, they applied improved sequential elastic components to lower the energy cost of walking on the ground level. Despite this, knee motors did not have a good effect on the knee joint during ground-level walking trials, necessitating the use of electrical power (8 W).

Ajayi et al. [11] used a bounded control and observer based controller. Utilized to calculate the angular position and angular velocities, which is then applied to the estimation of the joint torques. The convergence analysis of the high gain observer and the asymptotic stability of the bounded control law without human contribution were verified using Lyapunov based analysis, and fair path tracing of the physiotherapist's path was obtained.

Banala et al. [12] was developed a force-field controller in lower extremity rehabilitation. In order to the rehabilitation of patients sufferance from walking disability with active hip and knee joint and works in assistance as needed mode. Costa et al. [13] was presented a PID based controller to govern the activation of elevated power pneumatic muscle actuator for a lower limb orthosis with five degrees of freedom in each shank. It has to deal with the issue of nonlinearities that occur on occasion. Sherwani et al. [14] presented an adaptive Robust Integral of Sign Error (RISE) controller on the Exoskeleton Intelligently Communicating and Sensitive to Intention (EICoSI) to achieve optimal tracking error. Exoskeleton devices offered to help people with mobility problems can help their joints move more freely. RISE feedback is generally fused with adaptive controller, to enhance performance and lessen the high gain's effects. Chen et al. [15] used backstepping Adaptive Robust Control (ARC) algorithm for 1-DOF knee joint exoskeleton. The proposed ARC algorithm delivers guaranteed force tracking performance in both transient and steady-state conditions. They should note, that the suggested adaptive robust backstepping force controller not only provides a high level of robustness in the face of model uncertainty, but also provides faster closed loop responses and lower contact forces.

It can be concluded from previous studies that although much progress has been made in developing prosthetics and dealing with them with different control strategies. There are still a number of difficult problems in their precise control. Strong performance withinside the presence of parameter uncertainties, uncertain linearity, the influence of human

movement, and the control accuracy of reaction force should be considered in the control design of the prosthesis.

In this paper, it is proposed to use the Backstepping control strategy for a mathematical model of a system of Two Degrees of Freedom (2-DoF) that includes the thigh-leg. The Backstepping control tool is based on a control strategy that can be applied to a certain type of nonlinear system. The use of Lyapunov theory with Backstepping control maintains the closed-loop system's stability while also improving its dynamic performance. The Backstepping controller's design parameters have a direct impact on the controlled system's dynamic performance. As a result, selecting these design parameters is not an easy task, and if done incorrectly, instability issues will occur. The trial-and-error method of determining these parameters is difficult, time-consuming, and does not leading to an optimal solution in terms of the best dynamic performance. In order to improve dynamic performance regulation and tracking, the Bat Algorithm (BA) was utilized to adjust these parameters. This echolocation algorithm, which was inspired by bats, was first introduced by Yang [16].

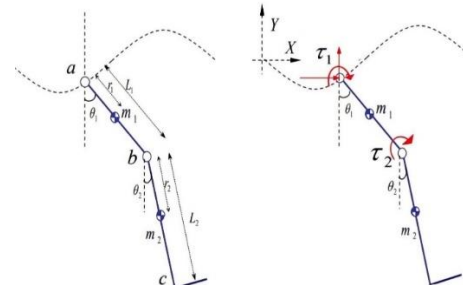
The aim of this research is how to design backstepping control to organize and control the tracking of desired walking paths while minimizing the effects of unknown disturbances, non-linear uncertainties in the system, and to ensure the stability of the system for the prosthetic knee.

## 2. DYNAMIC MODEL OF PROSTHETIC KNEE

Figure 1 (a) and 1(b) shows the human lower limb model and free body diagram of the prosthetic knee, the location of force effect on the prosthetic knee. The main objective is to derive the second order ordinary differential equations system. The motion of the prosthetic knee is controlled as a serial manipulator with rigid link, prosthetic knee can be modeled. In this case, it is easy to readily obtain the equations of motion. The method of Lagrangian can be used to obtain motion equation for a serial kinematic chain system [2].



(a) A person is wearing the prosthetic knee [17]



(b) Schematic diagram and free body diagram of the prosthetic knee

**Figure 1.** Prosthetic knee model

Axes involving the displacement of a prosthetic knee about a fixed axis should be established in a cartesian coordinate system and specify the sign and direction of the  $x$ -axis and  $y$ -axis, as shown in Figure 1b.

where  $X_1$  and  $Y_1$  are the displacements for the  $x$ - and  $y$ -axes for joint 1. In addition,  $X_2$  and  $Y_2$  are the displacements of the  $x$ -axis and  $y$ -axis for joint 2.

$$\left. \begin{aligned} X_1 &= r_1 \sin \theta_1 \\ Y_1 &= -r_1 \cos \theta_1 \\ X_2 &= L_1 \sin \theta_1 + r_2 \sin \theta_2 \\ Y_2 &= -L_1 \cos \theta_1 - r_2 \cos \theta_2 \end{aligned} \right\} \quad (1)$$

To derive the displacements in Eq. (1) with respect to time, the components of velocity are obtained as Eq. (2):

$$\left. \begin{aligned} \frac{d}{dt} X_1 &= r_1 \dot{\theta}_1 \cos \theta_1 \\ \frac{d}{dt} Y_1 &= r_1 \dot{\theta}_1 \sin \theta_1 \\ \frac{d}{dt} X_2 &= L_1 \dot{\theta}_1 \cos \theta_1 + r_2 \dot{\theta}_2 \cos \theta_1 \\ \frac{d}{dt} Y_2 &= L_1 \dot{\theta}_1 \sin \theta_1 + r_2 \dot{\theta}_2 \sin \theta_2 \end{aligned} \right\} \quad (2)$$

where,  $r_1$  and  $r_2$  are the distance between the center of mass of each link (thigh and shank),  $L_1$  is the length of link 1,  $\theta_1$  and  $\theta_2$  are the rotation angle of link 1 and link 2, respectively.

Langragian's equation is used in this analysis to determine the equation of motion, the mathematical formula to Langragian's equation can be written as follows [18]:

$$L = KE - PE \quad (3)$$

$$KE = \frac{1}{2} m v^2 \quad (4)$$

where,  $L$  is defined as the difference between the kinetic energy ( $KE$ ) and potential energy ( $PE$ ) of the mechanical system.

The  $KE$  equation is the summation of kinetic energy for individual links, and can be expressed by the following formula:

$$KE = \frac{1}{2} m_1 (\dot{X}_1^2 + \dot{Y}_1^2) + \frac{1}{2} I_1 \dot{\theta}_1^2 + \frac{1}{2} m_2 (\dot{X}_2^2 + \dot{Y}_2^2) + \frac{1}{2} I_2 \dot{\theta}_2^2 \quad (5)$$

where,  $I_1$  and  $I_2$  is the moment of inertia of the link 1 and link 2 (thigh and shank).

By substituting Eq. (2) into Eq. (5) to determine the total  $KE$  for two links:

$$\begin{aligned} KE &= \frac{1}{2} m_1 ((r_1 \dot{\theta}_1 \cos \theta_1)^2 + (r_1 \dot{\theta}_1 \sin \theta_1)^2) \\ &+ \frac{1}{2} (m_1 r_1^2 * \dot{\theta}_1^2) + \frac{1}{2} m_2 ((L_1 \dot{\theta}_1 \cos \theta_1 + r_2 \dot{\theta}_2 \cos \theta_2)^2 \\ &+ (L_1 \dot{\theta}_1 \sin \theta_1 + r_2 \dot{\theta}_2 \sin \theta_2)^2) + \frac{1}{2} (m_2 L_1^2 * \dot{\theta}_1^2) \end{aligned} \quad (6)$$

In addition,  $PE$  is the potential energy of system can be written as:

$$PE = -mgh \quad (7)$$

$$PE = -m_1 y_1 g - m_2 y_2 g \quad (8)$$

$$PE = m_1 r_1 g \cos \theta_1 - m_2 g (-L_1 \cos \theta_1 - r_2 \cos \theta_2) \quad (9)$$

Substitute Eq. (6) and Eq. (9) into Eq. (3), to get the following equation:

$$\begin{aligned} L &= \frac{1}{2} m_1 r_1^2 \dot{\theta}_1^2 + \frac{1}{2} I_1 \dot{\theta}_1^2 \\ &+ \frac{1}{2} m_2 (L_1^2 \dot{\theta}_1^2 + r_2^2 \dot{\theta}_2^2 + 2L_1 r_2 \dot{\theta}_1 \dot{\theta}_2 \cos(\theta_1 - \theta_2)) \\ &+ \frac{1}{2} I_2 \dot{\theta}_2^2 - m_1 r_1 g \cos \theta_1 - m_2 g L_1 \cos \theta_1 + m_2 g r_2 \cos \theta_2 \end{aligned} \quad (10)$$

The equations of motion for the manipulator are derived using the Lagrangian in Eq. (3) as the following:

$$\tau_{Total} = \frac{d}{dt} \left( \frac{\partial L}{\partial \dot{\theta}} \right) - \frac{\partial L}{\partial \theta} \quad (11)$$

where,  $i=1, 2$ , and  $\tau$  is torque acting on the system to each joint.

$$\begin{aligned} \frac{\partial L}{\partial \theta_1} &= -m_2 L_1 r_2 \dot{\theta}_1 \dot{\theta}_2 \sin(\theta_1 - \theta_2) + m_1 g r_1 \sin \theta_1 \\ &+ m_2 g L_1 \sin \theta_1 \end{aligned} \quad (12)$$

$$\begin{aligned} \frac{\partial L}{\partial \dot{\theta}_1} &= (I_1 + m_1 r_1^2 + m_2 L_1^2) \dot{\theta}_1 \\ &+ m_2 L_1 r_2 \dot{\theta}_2 \cos(\theta_1 - \theta_2) \end{aligned} \quad (13)$$

$$\begin{aligned} \frac{d}{dt} \left( \frac{\partial L}{\partial \dot{\theta}_1} \right) &= (I_1 + m_1 r_1^2 + m_2 L_1^2) \ddot{\theta}_1 + \\ &+ m_2 L_1 r_2 \dot{\theta}_2 \cos(\theta_1 - \theta_2) - m_2 L_1 r_2 \dot{\theta}_2 \sin(\theta_1 - \theta_2) (\dot{\theta}_1 - \dot{\theta}_2) \end{aligned} \quad (14)$$

$$\frac{\partial L}{\partial \theta_2} = -m_2 L_1 r_2 \dot{\theta}_1 \dot{\theta}_2 \sin(\theta_1 - \theta_2) + m_2 g r_2 \sin \theta_2 \quad (15)$$

$$\frac{\partial L}{\partial \dot{\theta}_2} = (m_2 r_2^2 + I_2) \dot{\theta}_2 + m_2 L_1 r_2 \dot{\theta}_1 \cos(\theta_1 - \theta_2) \quad (16)$$

$$\begin{aligned} \frac{d}{dt} \left( \frac{\partial L}{\partial \dot{\theta}_2} \right) &= (m_2 r_2^2 + I_2) \ddot{\theta}_2 + m_2 L_1 r_2 \dot{\theta}_1 \cos(\theta_1 - \theta_2) \\ &- m_2 L_1 r_2 \dot{\theta}_1 \sin(\theta_1 - \theta_2) (\dot{\theta}_1 - \dot{\theta}_2) \end{aligned} \quad (17)$$

The hip  $\tau_1$  and knee  $\tau_2$  torque expressions can be written as:

$$\begin{aligned} \tau_1 &= (I_1 + m_1 r_1^2 + m_2 L_1^2 - m_2 L_1 r_2 \cos(\theta_1 - \theta_2)) \ddot{\theta}_1 \\ &+ (m_2 r_2^2 + I_2 + m_2 L_1 r_2 \cos(\theta_1 - \theta_2)) \ddot{\theta}_2 - \\ &+ (m_2 L_1 r_2 \sin(\theta_1 - \theta_2)) \dot{\theta}_1^2 + (m_2 L_1 r_2 \sin(\theta_1 - \theta_2)) \dot{\theta}_2^2 \\ &- m_1 g r_1 \sin \theta_1 - m_2 g L_1 \sin \theta_1 \\ &- m_2 g r_2 \sin \theta_2 \end{aligned} \quad (18)$$

$$\begin{aligned} \tau_2 &= ((m_2 r_2^2 + I_2) \ddot{\theta}_2 + m_2 L_1 r_2 \dot{\theta}_1 \cos(\theta_1 - \theta_2) \\ &- m_2 L_1 r_2 \dot{\theta}_1^2 \sin(\theta_1 - \theta_2) \\ &- m_2 g r_2 \sin \theta_2 - L_1 \sin \theta_1 F_1 - L_2 \sin \theta_2 F_2) \end{aligned} \quad (19)$$

Assuming that there is no friction force, the dynamics model of the system can be expressed as general form below is [19].

$$M(\theta) \ddot{\theta} + C(\theta, \dot{\theta}) \dot{\theta} + G(\theta) = \tau \quad (20)$$

where,  $(\theta)$  is an angular position vector, which is expected to be usable by measurement,  $M(\theta)$  represents the inertia matrix of the links, while  $\tau$  is the control torque,  $C(\theta, \dot{\theta}) \dot{\theta}$  represents the vector of the Coriolis and centripetal torques, and  $G(\theta)$  represents gravitational torque.

Eq. (20) shows the nonlinear dynamics of the prosthetic knee system. The following can be represented using a state variable in the state equation:

$$\left. \begin{aligned} x_1 &= \theta_1, x_2 = \dot{\theta}_1 \\ x_3 &= \theta_2, x_4 = \dot{\theta}_2 \\ \dot{x}_1 &= \dot{\theta}_1, \dot{x}_2 = \ddot{\theta}_1, \dot{x}_3 = \dot{\theta}_2, \dot{x}_4 = \ddot{\theta}_2 \end{aligned} \right\} \quad (21)$$

where,  $[\theta_1, \theta_2]$  is angular position of upper and lower link.  $[\dot{\theta}_1, \dot{\theta}_2]$  represents angular velocity of upper and lower link [20].

Eq. (21) can be substituted into Eq. (20), which is a nonlinear dynamics equation, so Eq. (20) can be written as:

$$\dot{x}_1 = x_2 \quad (22)$$

$$\dot{x}_2 = \frac{1}{M_{11}}[\tau_1 - M_{12}\dot{x}_4 - C_1x_2 - G_1] \quad (23)$$

$$\dot{x}_3 = x_4 \quad (24)$$

$$\dot{x}_4 = \frac{1}{M_{22}}[\tau_2 - M_{21}\dot{x}_2 - C_2x_4 - G_2] \quad (25)$$

Figure 2 shows the MATLAB/SIMULINK of the prosthetic knee model. To simulate the prosthetic knee model representation by using Eq. (22)-(25). Table 1 exhibits the model of prosthetic knee parameters values that utilized in the simulation.

**Table 1.** Physical parameters values of the prosthetic knee [21]

Prosthetic knee parameters	Parameter value
$m_1$	5.28 kg
$m_2$	2.23 kg
$I_1$	0.033 kg.m <sup>2</sup>
$I_2$	0.033 kg.m <sup>2</sup>
$L_1$	0.302 m
$L_2$	0.332 m
$r_1$	0.236 m
$r_2$	0.189 m
$g$	9.81 m/s <sup>2</sup>

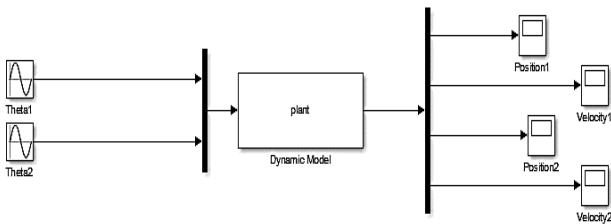


**Figure 2.** Open loop prosthetic knee system represented by MATLAB SIMULINK

Figure 3 represents the results of the open loop trajectory and the speed with which the prosthesis moves within the initial conditions ( $\theta=10^\circ$ ) [22]. The main problem is the instability and controllability of the movement of the prosthesis resulting from the lack of control over the location and speed which will certainly lead to undesirable movement of the limb which in turn must be controlled. Clearly from Figure 3, the open loop system is unstable. Consequently, the Backstepping controller is utilized to stabilized the prosthetic

knee and make its states reach the asymptotically stable region with maximal angle.

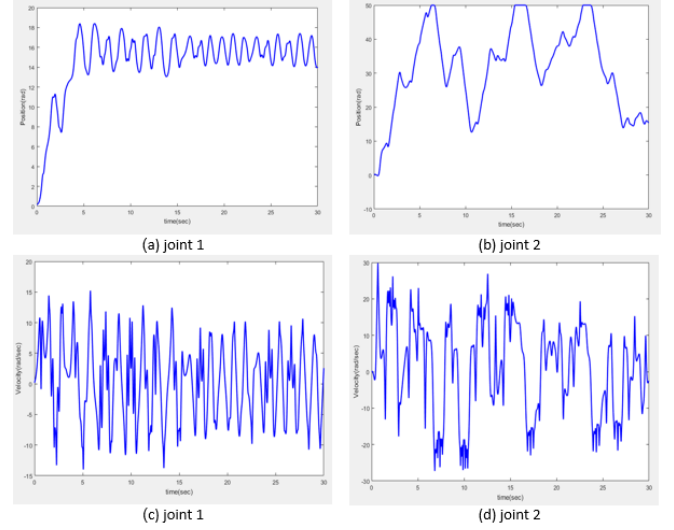


**Figure 3.** Open loop response of prosthesis knee, (a, and b) represents position of link 1 and 2, in addition to (c, and d) is the velocity of link 1 and link 2

### 3. BACKSTEPPING CONTROLLER DESIGN

The backstepping approach provides a systematic method for designing a control structure to monitor a reference signal. Suggested Backstepping to control the lower prosthesis as the dynamic model is based on this approach. The controller is introduced which ensures convergent stability in tracking the desired position and speed trajectories. The control laws are derived from Lyapunov theory-based stability assessments of the Backstepping controller to control the prosthesis knee [23, 24].

In order to create the Backstepping control algorithm for a prosthetic knee system, follow the procedures listed [25].

Steps 1: Suppose that the error  $e_1$ , represents the actual stat  $x_1$  and intended trajectory  $x_{d1}$  described by the

$$e_1 = x_1 - x_{d1} \quad (26)$$

The time derivative of the error in Eq. (26), the tracking velocity, can be written as follows:

$$\dot{e}_1 = \dot{x}_1 - \dot{x}_{d1} \quad (27)$$

Defining the first virtual control  $\alpha_1=x_2$  and sub in Eq. (27) to get:

$$\dot{e}_1 = \alpha_1 - \dot{x}_{d1} \quad (28)$$

The positive Lyapunov function:

$$V_1 = \frac{1}{2}e_1^2 \quad (29)$$

The Lyapunov functions derivative during time is called:

$$\dot{V}_1 = e_1\dot{e}_1 \quad (30)$$

As follows: by substituting Eq. (28) into Eq. (30) to gate a new derivative of the Lyapunov function, which can be written as follows:

$$\dot{V}_1 = e_1(\alpha_1 - \dot{x}_{d1}) \quad (31)$$

A virtual control is created ( $\alpha_1 = -c_1 e_1 + \dot{x}_{d1}$ ), and sub it into Eq. (31) then:

$$\dot{V}_1 = -c_1 e_1^2 \quad (32)$$

This means that  $\dot{V}_1 < 0$ .

Let the error  $e_2$ , between actual state  $x_2$  and the first virtual control  $\alpha_1$  described by:

$$e_2 = x_2 - \alpha_1 \quad (33)$$

Taking the time derivative of Eq. (33) and using Eq. (23) to get:

$$\dot{e}_2 = \frac{1}{M_{11}}[\tau_1 - M_{12}\dot{x}_4 - C_1 x_2 - G_1] + \alpha_1 \quad (34)$$

The second Lyapunov function is  $V_2 = \frac{1}{2}e_1^2 + \frac{1}{2}e_2^2$ .

Using the time derivative of Lyapunov function and the presumption that ( $\alpha_1 = -c_1 e_1 + \dot{x}_{d1}$ ) to get:

$$\dot{V}_2 = -c_1 e_1^2 + e_2(e_1 + (\frac{1}{M_{11}}[\tau_1 - M_{12}\dot{x}_4 - C_1 x_2 - G_1]) + c_1 \dot{e}_1 - \dot{x}_{d1}) \quad (35)$$

Choosing the first control law:

$$\tau_1 = M_{11}[-e_1 - c_1 \dot{e}_1 - c_2 e_2 + \dot{x}_{d1}] + M_{12}\dot{x}_4 + C_1 x_2 + G_1 \quad (36)$$

The derivative of Lyapunov function leads to:

$$\dot{V}_2 = -c_1 e_1^2 - c_2 e_2^2 \quad (37)$$

where,  $c_1$  and  $c_2$  are a positive constant to be determined using Bat algorithm, and  $\dot{V}_2 < 0$  are negative definite.

Step 2: Let  $e_3$ , represent the actual state  $x_3$  of the desired trajectory  $x_{d3}$  as defined by:

$$e_3 = x_3 - x_{d3} \quad (38)$$

The time derivative of Eq. (38), and in addition to assigning the second virtual control ( $\alpha_2 = \dot{x}_3$ ) in order to get the error of the tracking velocity, it is written as follows:

$$\dot{e}_3 = \alpha_2 - \dot{x}_{d3} \quad (39)$$

By using third Lyapunov function:

$$V_3 = V_2 + \frac{1}{2}e_3^2 \quad (40)$$

Since the time derivative of  $V_3$  is given by:

$$\dot{V}_3 = \dot{V}_2 + e_3 \dot{e}_3 \quad (41)$$

Using Eq. (39) and Eq. (41) to get:

$$\dot{V}_3 = -c_1 e_1^2 - c_2 e_2^2 + e_3(\alpha_2 - \dot{x}_{d3}) \quad (42)$$

By substitution, the virtual control ( $\alpha_2 = -c_3 e_3 + \dot{x}_{d3}$ ) in to  $\dot{V}_3$  to equation becomes:

$$\dot{V}_3 = -c_1 e_1^2 - c_2 e_2^2 - c_3 e_3^2 \quad (43)$$

Step 3: Consider the error  $e_4$  as a representation of  $x_4$  and the second virtual control  $\alpha_2$  as:

$$e_4 = x_4 - \alpha_2 \quad (44)$$

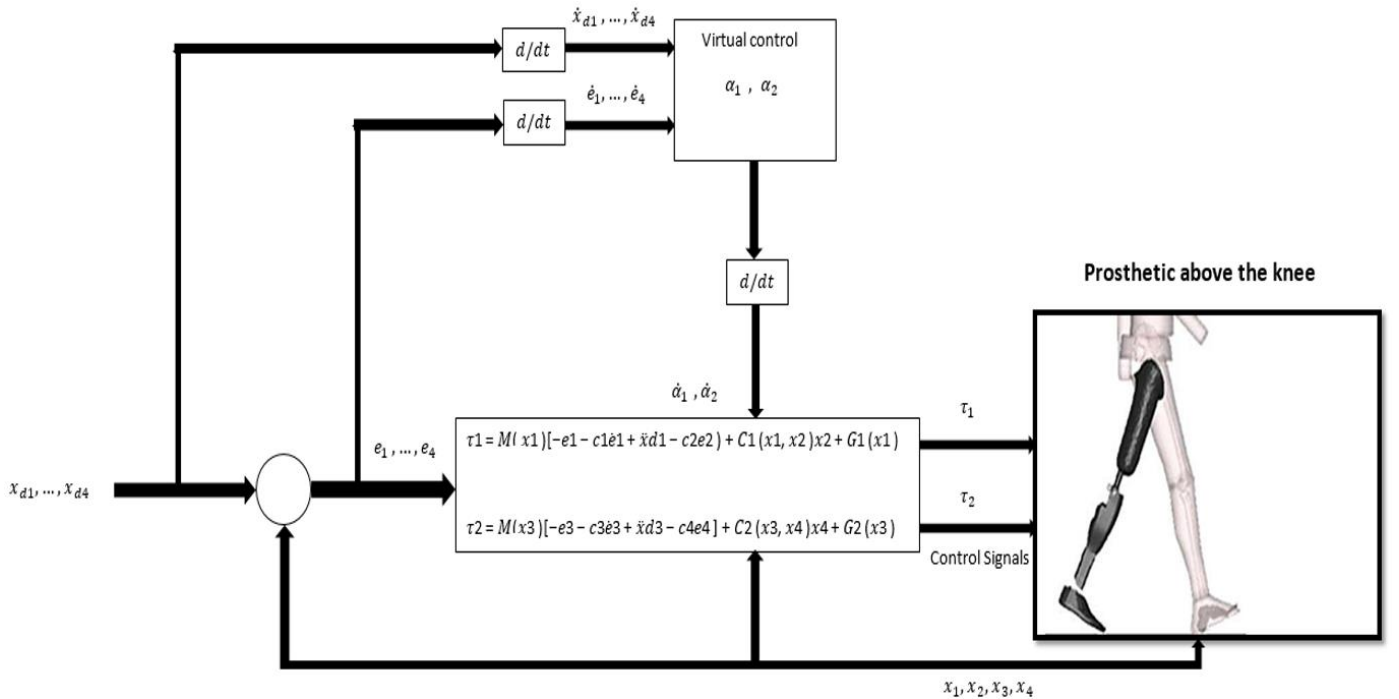


Figure 4. Backstepping control for a prosthetic knee

The time derivative of the error  $e_4$ , and Sub  $\dot{x}_4$  from Eq. (25) to get:

$$\dot{e}_4 = \frac{1}{M_{22}}[\tau_2 - M_{21}\dot{x}_2 - C_2x_4 - G_2] - \alpha_2 \quad (45)$$

Using fourth Lyapunov function:

$$V_4 = V_3 + \frac{1}{2}e_4^2 \quad (46)$$

Taking the time derivative of Lyapunov function, and compensation Eq. (43) and Eq. (45):

$$\dot{V}_4 = -c_1e_1^2 - c_2e_2^2 - c_3e_3^2 + e_4(e_3 + [\frac{1}{M_{22}}[\tau_2 - M_{21}\dot{x}_2 - C_2x_4 - G_2]c_3\dot{e}_3 - \ddot{x}_{d3}]) \quad (47)$$

Choosing the second control law:

$$\tau_2 = M_{22}[-e_3 - c_3\dot{e}_3 - c_4e_4 + \ddot{x}_{d3}] + M_{21}\dot{x}_2 + C_2x_4 + G_2 \quad (48)$$

The derivative of Lyapunov function leads to:

$$\dot{V}_4 = -c_1e_1^2 - c_2e_2^2 - c_3e_3^2 - c_4e_4^2 \quad (49)$$

As a result, the selection of control law  $\tau_2$  assures that  $\dot{V}_4$  to be negative definite, ensuring the whole system's asymptotic stability characteristics. Figure 4 shows a schematic design of backstepping control for lower limb prosthesis.

#### 4. OPTIMAL BACKSTEPPING CONTROL PARAMETERS

All control systems must have minimal error, good steady-state and transient performance. Parameters of the backstepping algorithm have an effect on the system's output and stability. These four design parameters are designated as  $c_1$ ,  $c_2$ ,  $c_3$ , and  $c_4$  in this study utilizing the BAT method to discover the best value of parameter control for the prosthetic knee. BAT is inspired by the echolocation conduct of common bats for figuring out their food, is proposed in the refs. [16, 26]. Bats make loud noises in order to detect possible prey. This signal returns after it collides with an object. They can quickly receive or analyze the signals and forecast the object's size and moving direction. Using the following assumptions, echolocation properties of bats will be generated to resolve the optimization problem [27]:

(1) Echolocation is used by all bats to determine distance.

(2) Bats fly with random velocities  $V_i$ , at position  $X_i$ , at a set frequency  $f_{min}$ , varying wavelength  $\lambda$  and loudness  $A_0$  to locate prey. They set their (wavelength/frequency) and can regulate pulse emission rate  $r \in [0-1]$  based on their prey's proximity.

(3) The loudness can change in many ways we assume that the loudness changes from a large (positive)  $A_0$  to a minimum constant value  $A_{min}$ .

In addition to the above principles, frequency and wavelengths occur within the range of  $[f_{min}, f_{max}]$  and  $[\lambda_{min}, \lambda_{max}]$  respectively in practical applications, is chosen in such a way that it closely resembles the dimensions of the area of interest. In order to solve an optimization problem with a virtual bat, rules must be created to determine their positions and velocities in the d-dimensional study space. At time step t, the

new position  $X_i^t$  it and velocity  $V_i^t$  it is defined as follows:

$$f_i = f_{min} + (f_{max} - f_{min})\beta \quad (50)$$

$$V_i^t = V_i^{t-1} + (X_i^t - X_*)f_i \quad (51)$$

$$X_i^t = X_i^{t-1} + V_i^t \quad (52)$$

here,  $\beta \in [0-1]$  is the random vector taken from a uniformly distribute;  $X_*$  denotes the current global best location (solution) as determined by a comparison of all solutions for all n bats.

Once a solution is chosen from among the actual better options for the local research, a new solution for each bat is developed locally utilizing random walk.

$$X_{new} = X_{old} + \epsilon A^t \quad (53)$$

When a bat locates its prey, the sound level drops and the rate of pulse emission rises. The bat is heading to the optimal solution according to:

$$A_i^{t+1} = \alpha A_i^t, r_i^{t+1} = r_i^0 [1 - e^{-\gamma t}] \quad (54)$$

here,  $\alpha$  and  $\gamma$  are constant ( $\alpha = \gamma = 0.9$ ), the initial emission rate is  $r_0 \in [0-1]$ , and the initial loudness is  $A_i \in [0.1-0.9]$ .

BAT algorithms is used for tuning the  $[c_1, c_2, c_3, c_4]$  parameters of the proposed controller for a prosthesis knee. At the end of the algorithm, the optimal values of design parameters are set and discovered to the Backstepping controller. The BA has set the maximum number of iterations to 100 and the population size to 40. The cost function that used to evaluate each particle during the search of minimal is chosen to be the Mean Square Error (MSE) given by:

$$MSE = \frac{1}{n} \sum_{t=1}^n e_1(i)^2 + \frac{1}{n} \sum_{t=1}^n e_3(i)^2 \quad (55)$$

where,  $e_1 = x_1 - x_{d1}$  and  $e_3 = x_3 - x_{d3}$ ,  $n$  is the sampling numbers. Figure 5 shows the cost function's behavior as a function of algorithm iterations.

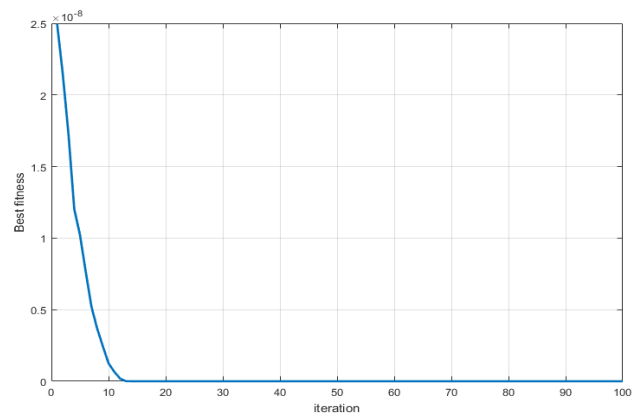


Figure 5. BAT cost function

Table 2. Optimal values of design parameters

Parameters	Value
$c_1$	328.16
$c_2$	476.397
$c_3$	332.181
$c_4$	520.836

Backstepping design parameters optimized using the BAT method are shown in Table 2. Finally, the Backstepping controller sets these optimal values in order to achieve a system controlled by optimal Backstepping control.

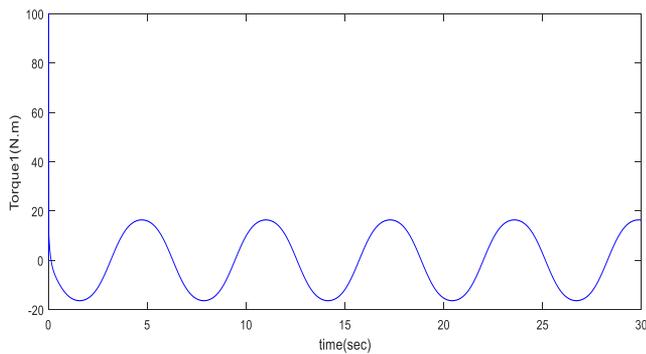
### 5. SIMULATION RESULTS

A Backstepping controller designed for prosthetic knee stabilization, tracking, and regulatory control is described in this section. A MATLAB/SIMULINK simulation is used to evaluate the controller and analyze the performance of the backstepping controlled system. As shown in Table 1, the values of the system parameters for a prosthetic knee with a 2-DOF joint are provided. To compare between the performances of Backstepping controllers due to try-and-error method and Bat algorithm, the Mean Square Error (MSE) has been used as a metric for evaluating performance. The Optimal and Trial-and-Error values of the controller design parameters are listed in Table 3.

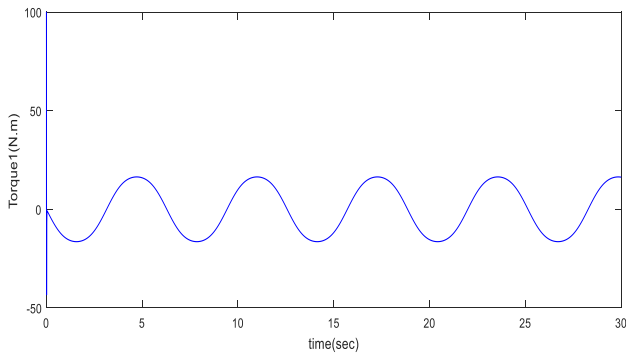
**Table 3.** Optimal and Trial-and-Error values of the controller design parameters

Design parameters	Optimal value	Trial-and-Error value
$c_1$	328.16	9
$c_2$	476.397	9
$c_3$	332.181	9
$c_4$	520.836	9

Figures 6 and 7 presents the control signal for both joints by applying the Backstepping control approach. According to the figures, despite system nonlinearity and parameter variation, the controlled system tracks the desired trajectory.

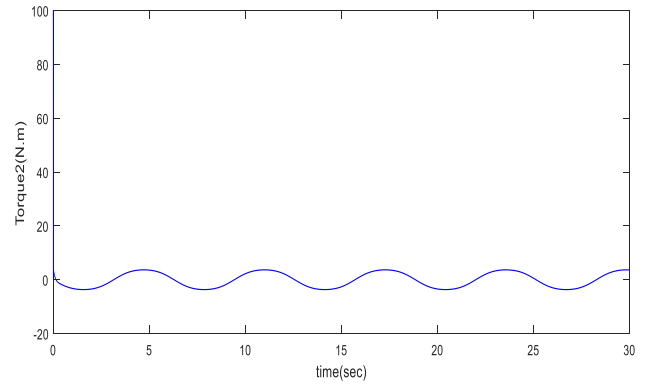


(a) Backstepping control

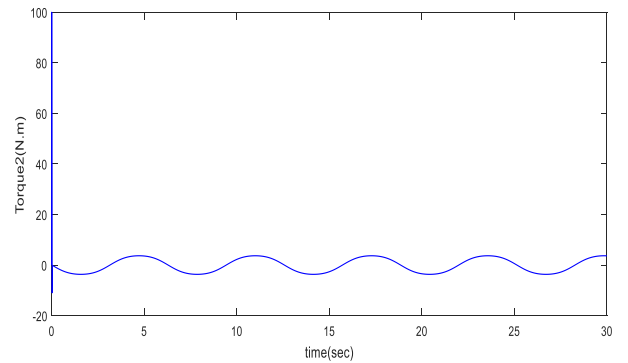


(b) Optimal Backstepping control

**Figure 6.** Control signal applied to the first joint



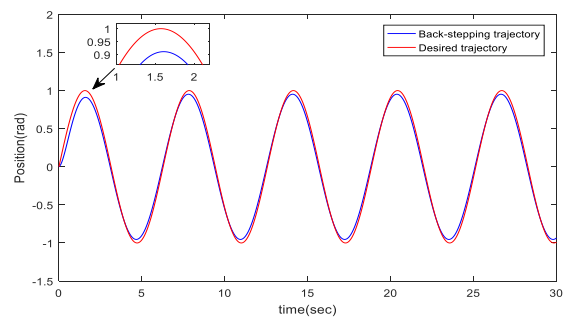
(a) Backstepping control



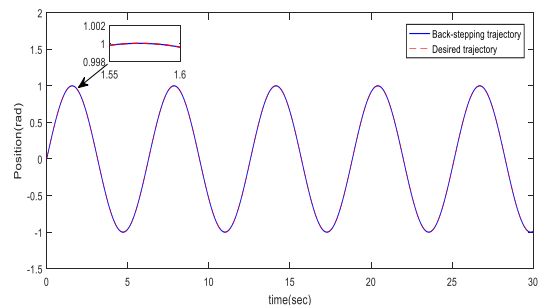
(b) Optimal Backstepping control

**Figure 7.** Control signal applied to the second joint

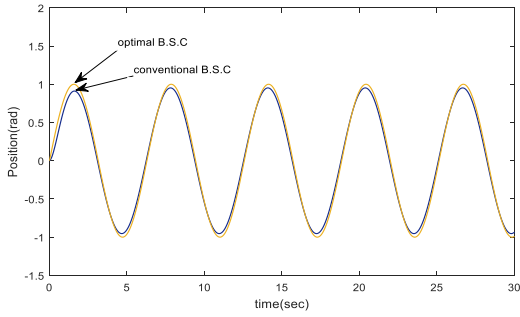
The experimental validation results are compared to the results acquired through the use of the Backstepping controller and bat algorithms. In fact, found that, the system has a high level of stability and good convergence in a limited time. In terms of the results of the position tracking, Figure 8 and 9 shows that the proposed Backstepping control with bat algorithms scheme ameliorates considerably the position tracking compared to the Backstepping control. In addition, using bat algorithms the tracking position error was strongly decreased.



(a) Backstepping control

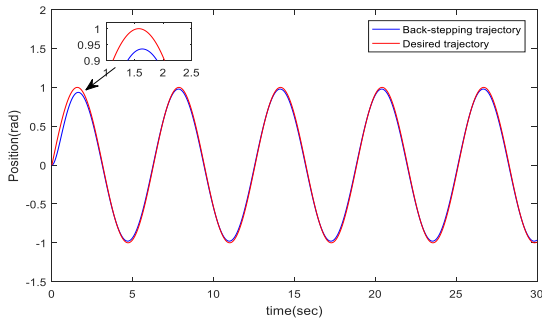


(b) Optimal Backstepping control

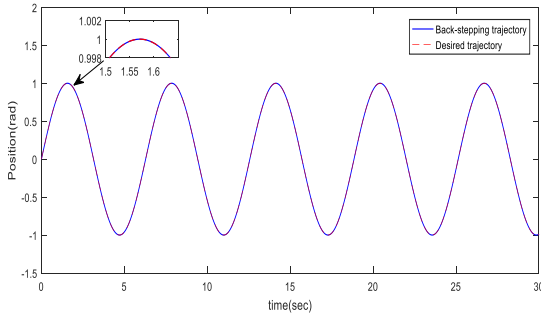


(c) Compare between optimal and conventional Backstepping control

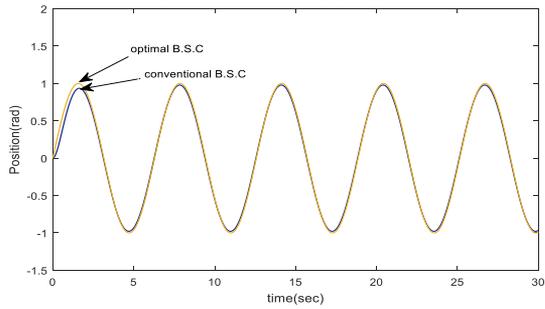
**Figure 8.** Position trajectory for joint 1



(a) Backstepping control



(b) Optimal Backstepping control

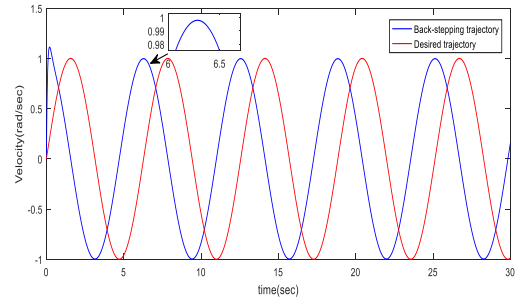


(c) Compare between optimal and conventional Backstepping control

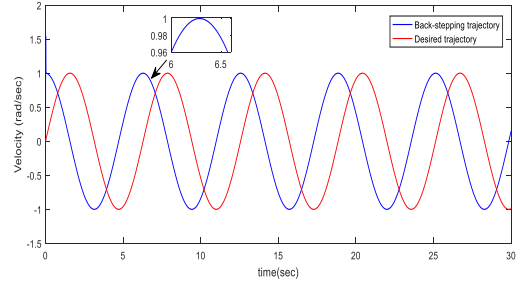
**Figure 9.** Position trajectory for joint 2

For the position tracking trajectory, the maximum tracking error of the joint1 is equal to 9% at peak, and the maximum tracking error of the joint2 is equal to 7.4% at peak for the backstepping controller. As a consequence, a thorough examination of the results that the optimal Backstepping control scheme decreases tracking errors by a factor of 0% for both position in joint1 and joint2. Moreover, the velocity tracking errors shown in Figure 10 and 11 that using Backstepping control with bat algorithms is better for

enhances greatly the tracking performance. From Figures 10 and 11 showed that there is a high tracking velocity with bat algorithms for the desired trajectory.

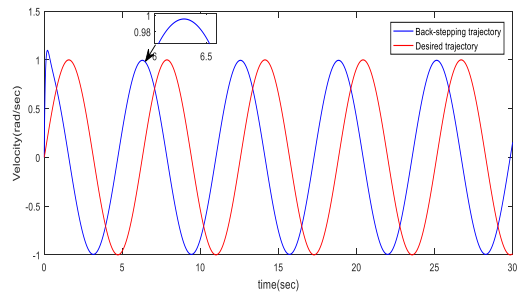


(a) Backstepping control

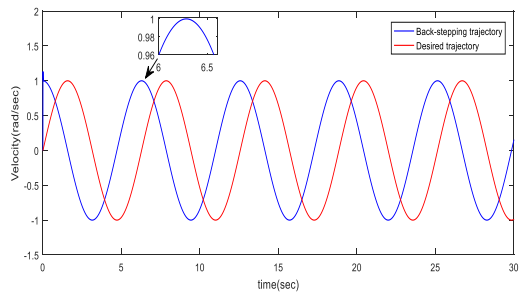


(b) Optimal Backstepping control

**Figure 10.** Velocity trajectory for joint 1

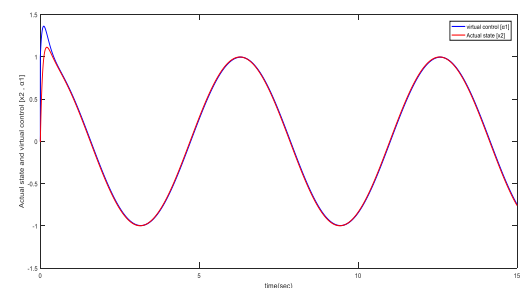


(a) Backstepping control

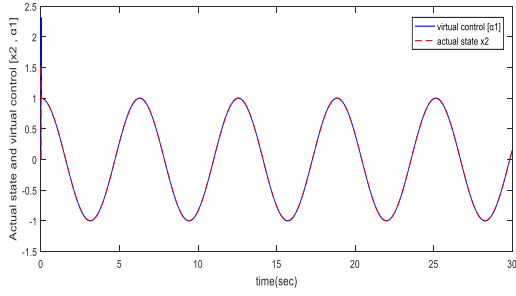


(b) Optimal Backstepping control

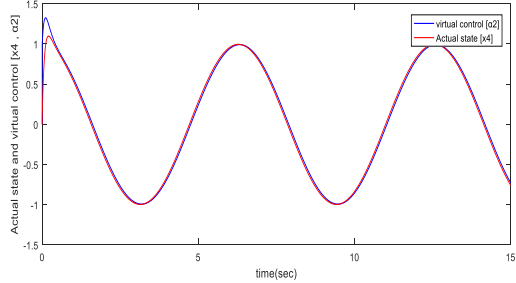
**Figure 11.** Velocity trajectory for joint 2



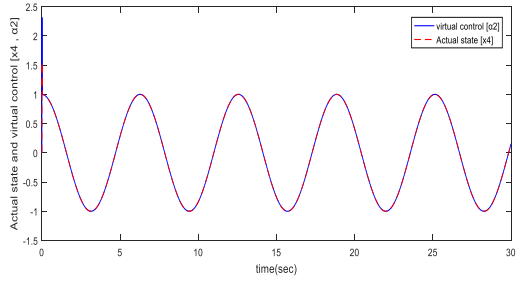
(a) joint1



(b) joint2

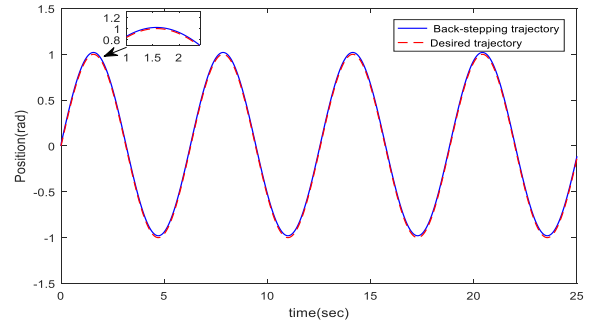


(c) joint1

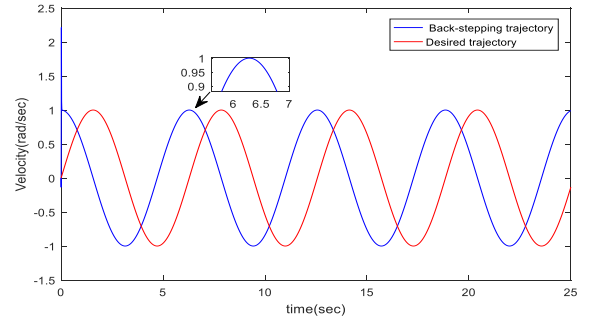


(d) joint2

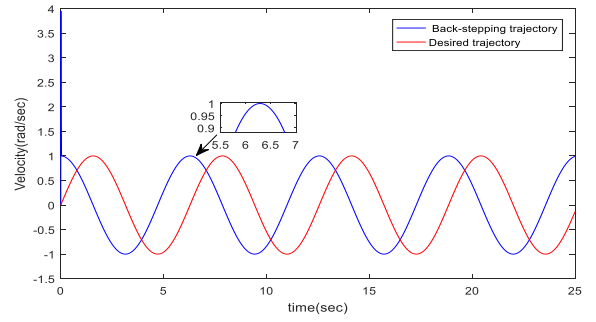
**Figure 12.** Behavior of actual and virtual states: (a) and (c) backstepping control. (b) and (d) Optimal Backstepping control



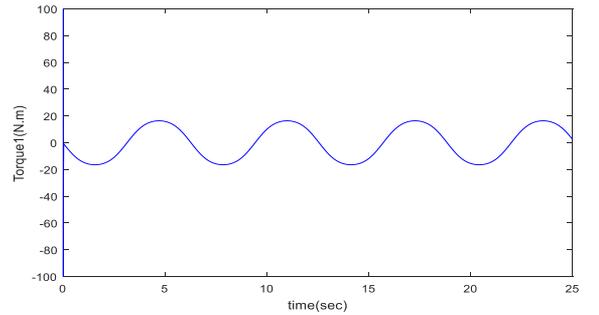
(b) joint2



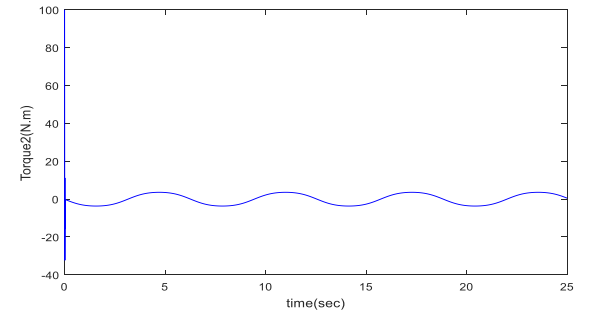
(c) joint1



(d) joint2

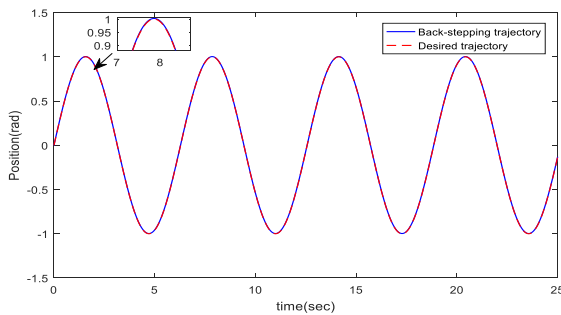


(e) joint1



(f) joint1

**Figure 13.** Comparison between position, velocity and control signal for joint 1 and joint 2 with external disturbances



(a) joint1

Figure 12 shows how actual and virtual states behave. The figures show how well the virtual states track and correlate to their physical counterparts in the end.

The parameters of the prosthetic knee in Table 1 are used in the model with the Backstepping controlled system. The results are compared with Mefoued et al. [8]. In Figure 13, perturbations are applied on a resistive torque (disturbance)  $d_1=200$ , and  $d_2=400$  because with time the parameters values will be changed slightly or the system suffering from external disturbances. This percentage of the uncertainty is our case study. Found that the results prove both joint1 and joint2 trajectories follow the desired trajectory with a high performance. It can be concluded that the proposed Backstepping control is more robust against this perturbation.

## 6. CONCLUSIONS

In this paper presented to design and developed for a 2-DOF prosthetic knee using the Backstepping approach, a new state is added to the system's equations. The two control laws are generated to be responsible to give good track of desired trajectory for the both joint1 and joint 2. The effectiveness of this control scheme has been verified by simulation on MATLAB 2019b. The simulation findings were compared to those published in earlier publications on sliding mode control to ensure they were accurate. To prevent the need for a trial-and-error approach for tuning the design Backstepping control, Bat algorithm is applied to determine optimal design parameters in terms of improved better dynamic performance. Therefore, the proposed Backstepping controller with BA results showed that the position error of the prosthetic knee is enhanced by 9% at joint1 and 7.4% at joint 2, when it is compared with backstepping control by used try-and-error parameters.

## REFERENCES

- [1] Zhang, X., Li, J., Hu, Z., Qi, W., Zhang, L., Hu, Y., Su, H., Ferrigno, G., Momi, E.D. (2019). Novel design and lateral stability tracking control of a four-wheeled rollator. *Applied Sciences*, 9(11): 2327. <https://doi.org/10.3390/app9112327>
- [2] Borjian, R. (2008). Design, modeling, and control of an active prosthetic knee. Master's thesis, University of Waterloo.
- [3] Tucker, M.R., Olivier, J., Pagel, A., Bleuler, H., Bourli, M., Lamercy, O., Millán, J., Riener, R., Vallery, H., Gassert, R. (2015). Control strategies for active lower extremity prosthetics and orthotics: A review. *Journal of Neuroengineering and Rehabilitation*, 12(1): 1-30. <https://doi.org/10.1186/1743-0003-12-1>
- [4] Li, Z., Huang, B., Ajoudani, A., Yang, C., Su, C.Y., Bicchi, A. (2017). Asymmetric bimanual control of dual-arm exoskeletons for human-cooperative manipulations. *IEEE Transactions on Robotics*, 34(1): 264-271. <https://doi.org/10.1109/TRO.2017.2765334>
- [5] Thamir, L., Khazaal, M. (2021). Design of an optimal backstepping controller for nonlinear system under disturbance. *Engineering and Technology Journal*, 39(3): 465-476. <http://dx.doi.org/10.30684/etj.v39i3A.1801>
- [6] Azimi, V., Shu, T., Zhao, H., Ambrose, E., Ames, A.D., Simon, D. (2017). Robust control of a powered transfemoral prosthesis device with experimental verification. In 2017 American Control Conference (ACC), Seattle, WA, USA, pp. 517-522. <https://doi.org/10.23919/ACC.2017.7963005>
- [7] Scandaroli, G.G., Borges, G.A., da Rocha, A.F., de Oliveira Nascimento, F.A. (2008). Adaptive knee joint control for an active amputee prosthesis. In 2008 IEEE Latin American Robotic Symposium, Salvador, Brazil, pp. 164-169. <https://doi.org/10.1109/LARS.2008.12>
- [8] Mefoued, S., Belkhiat, D.E.C. (2019). A robust control scheme based on sliding mode observer to drive a knee-exoskeleton. *Asian Journal of Control*, 21(1): 439-455. <https://doi.org/10.1002/asjc.1950>
- [9] Wen, Y., Liu, M., Si, J., Huang, H.H. (2016). Adaptive control of powered transfemoral prostheses based on adaptive dynamic programming. In 2016 38th Annual International Conference of the IEEE Engineering in Medicine and Biology Society (EMBC), Orlando, FL, pp. 5071-5074. <https://doi.org/10.1109/EMBC.2016.7591867>
- [10] Martinez-Villalpando, E.C., Herr, H. (2009). Agonist-antagonist active knee prosthesis: A preliminary study in level-ground walking. *Journal of Rehabilitation Research & Development*, 46(3): 361-374. <https://doi.org/10.1682/JRRD.2008.09.0131>
- [11] Ajayi, M.O., Djouani, K., Hamam, Y. (2017). Bounded control of an actuated lower-limb exoskeleton. *Journal of Robotics*, Article ID: 2423643. <https://doi.org/10.1155/2017/2423643>
- [12] Banala, S.K., Kim, S.H., Agrawal, S.K., Scholz, J.P. (2008). Robot assisted gait training with active leg exoskeleton (ALEX). *IEEE Transactions on Neural Systems and Rehabilitation Engineering*, 17(1): 2-8. <https://doi.org/10.1109/TNSRE.2008.2008280>
- [13] Costa, N., Bezdicek, M., Brown, M., Gray, J.O., Caldwell, D.G., Hutchins, S. (2006). Joint motion control of a powered lower limb orthosis for rehabilitation. *International Journal of Automation and Computing*, 3(3): 271-281. <https://doi.org/10.1007/s11633-006-0271-x>
- [14] Sherwani, K.I., Kumar, N., Chemori, A., Khan, M., Mohammed, S. (2020). RISE-based adaptive control for EICoSI exoskeleton to assist knee joint mobility. *Robotics and Autonomous Systems*, 124: 103354. <https://doi.org/10.1016/j.robot.2019.103354>
- [15] Chen, S., Yao, B., Zhu, X., Chen, Z., Wang, Q., Zhu, S., Song, Y. (2015). Adaptive robust backstepping force control of 1-DOF joint exoskeleton for human performance augmentation. *IFAC-Papers OnLine*, 48(19): 142-147. <https://doi.org/10.1016/j.ifacol.2015.12.024>
- [16] Yang, X.S. (2010). A new metaheuristic bat-inspired algorithm. In *Nature Inspired Cooperative Strategies for Optimization (NICSO 2010)*, pp. 65-74. [https://doi.org/10.1007/978-3-642-12538-6\\_6](https://doi.org/10.1007/978-3-642-12538-6_6)
- [17] Lawson, B.E., Mitchell, J., Truex, D., Shultz, A., Ledoux, E., Goldfarb, M. (2014). A robotic leg prosthesis: Design, control, and implementation. *IEEE Robotics & Automation Magazine*, 21(4): 70-81. <https://doi.org/10.1109/MRA.2014.2360303>
- [18] Ali, H.I., Hasan, A.F., Jassim, H.M. (2020). Optimal h2pid controller design for human swing leg system using cultural algorithm. *Journal of Engineering Science and Technology*, 15(4): 2270-2288.
- [19] Ali, H.I., Kadhim, M.J. (2018). Mixed H<sub>2</sub>/Sliding mode controller design for human swing leg system. In 2018 Third Scientific Conference of Electrical Engineering (SCEE), Baghdad, Iraq, pp. 156-161. <https://doi.org/10.1109/SCEE.2018.8684215>
- [20] Ali, S.S., Raafat, S.M., Al-Khazraji, A. (2020). Improving the performance of medical robotic system using H<sub>∞</sub> loop shaping robust controller. *International Journal of Modelling, Identification and Control*, 34(1): 3-12. <https://doi.org/10.1504/IJMIC.2020.108911>
- [21] Mu, X., Wu, Q. (2003). A complete dynamic model of five-link bipedal walking. In *Proceedings of the 2003 American Control Conference*, Denver, CO, USA, pp. 4926-4931. <https://doi.org/10.1109/ACC.2003.1242503>
- [22] Goldberg, S.R., Öunpuu, S., Delp, S.L. (2003). The importance of swing-phase initial conditions in stiff-knee

- gait. *Journal of Biomechanics*, 36(8): 1111-1116. [https://doi.org/10.1016/S0021-9290\(03\)00106-4](https://doi.org/10.1016/S0021-9290(03)00106-4)
- [23] Mohammad, A.M., AL-Samarraie, S.A. (2020). Robust controller design for flexible joint based on backstepping approach. *Iraqi Journal of Computers, Communications, Control and Systems Engineering*, 20(2): 58-73.
- [24] Zhang, D., Du, B., Zhu, P., Wu, W. (2020). Adaptive backstepping sliding mode control of trajectory tracking for robotic manipulators. *Complexity*, Article ID 3156787. <https://doi.org/10.1155/2020/3156787>
- [25] Humaidi, A.J., Kadhim, S.K., Gataa, A.S. (2020). Development of a novel optimal backstepping control algorithm of magnetic impeller-bearing system for artificial heart ventricle pump. *Cybernetics and Systems*, 51(4): 521-541. <https://doi.org/10.1080/01969722.2020.1758467>
- [26] Yang, X.S. (2011). Bat algorithm for multi-objective optimisation. *International Journal of Bio-Inspired Computation*, 3(5): 267-274. <https://doi.org/10.1504/IJBIC.2011.042259>
- [27] Hussin, K.N., Nahar, A.K., Khleaf, H.K. (2021). A visual enhancement quality of digital medical image based on bat optimization. *Engineering and Technology Journal*, 39(10): 1550-1570. <http://dx.doi.org/10.30684/etj.v39i10.2165>